Magnetic Circular Dichroism and Electron Paramagnetic Resonance Studies of Iron(II)–Metallothionein†

Mark T. Werth and Michael K. Johnson*
School of Chemical Sciences and Center for Metalloenzyme Studies, University of Georgia, Athens, Georgia 30602
Received November 22, 1988; Revised Manuscript Received January 23, 1989

ABSTRACT: The electronic and magnetic properties of the Fe(II)–thiolate centers in Fe(II)–metallothionein have been investigated by low-temperature magnetic circular dichroism and electron paramagnetic resonance spectroscopies at various levels of Fe(II) incorporation. In agreement with previous results [Good, M., & Vašák, M. (1986) *Biochemistry 25*, 8353–8356], rabbit liver metallothionein was found to bind a maximum of seven Fe(II) ions, with cluster formation occurring when more than four Fe(II) ions are bound at pH 8.5. The results indicate that all the iron in fully loaded Fe(II)–metallothionein is accommodated in Fe(II)–thiolate clusters that have either $S = 0$ or $S = 2$ ground states as a result of antiferromagnetic coupling between high-spin Fe(II) ions. By analogy with the cluster composition and mechanism of assembly that have been established for other divalent metal ions, the clusters with $S = 0$ and $S = 2$ ground states are attributed to tetranuclear and trinuclear centers, respectively. EPR signals indicative of $S = 2$ species were observed for samples containing monomeric tetrathiolate–Fe(II) centers and trinuclear Fe(II)–thiolate clusters. However, the nature of the zero-field splitting of the $S = 2$ ground states that is indicated by the EPR signals is not consistent with that deduced from Mössbauer and magnetic circular dichroism studies, suggesting heterogeneity in both types of center.

Metallothioneins (MT's)[1] are a class of metal binding proteins which, since their discovery in 1957 (Margoshes & Vallee, 1957), have been found to be widely distributed in nature (Nordberg & Kojima, 1979; Kägi et al., 1984). The specific biological function(s) of these ubiquitous proteins are still largely unknown. However, they are capable of binding a wide range of metal ions, including Co(II), Ni(II), Cu(I), Au(I), Ag(I), Zn(II), Cd(II), Hg(II), Bi(III), In(III), Sb(III), and Pb(II) (Hamer, 1985; Nielson et al., 1985), suggesting a role in trace metal metabolism. In addition, the biosynthesis of MT's is induced by high levels of Cd^{2+}, Zn^{2+}, and Cu^{1+} (Nordberg & Kojima, 1979), a result which implies involvement in heavy metal detoxification. The early discovery of MT in equine renal tissue prompted the proposal that MT was involved in intracellular iron metabolism (Kägi & Vallee, 1961). However, given the abundance of iron in biology, there have been surprisingly few studies of iron binding to MT.

Clear evidence that metallothionein is capable of binding iron has only recently emerged (Good & Vašák, 1986). By use of a combination of UV–visible, near-infrared, and room temperature magnetic circular dichroism (MCD)[1] spectroscopies, apometallothionein (apoMT)[1] from rabbit liver was found to bind up to seven Fe(II) ions, each tetrahedrally coordinated by thiolate sulfur. Mammalian MT's (M_r = 6000–7000) typically contain 20 cysteine residues out of 61–62 total amino acid residues (Kojima et al., 1976). Thus, in fully loaded Fe(II)–MT, the cysteine thiolate to iron ratio is 2.86. In order to achieve tetrahedral thiolate coordination, it is clear that some of the cysteine thiolate ligands must adopt a doubly bridging mode of coordination. In accord with this observation, Good and Vašák observed a progressive red shift in the S → Fe(II) charge-transfer transition for Fe(II)/apoMT ratios greater than 4, which they interpreted in terms of the formation of metal–thiolate clusters with doubly bridging thiolate coordination.

The nature and assembly of metal–thiolate clusters in Cd_7– and Zn_2Cd_5–mammalian MT has been extensively studied [for a recent review, see Vašák (1988)]. In particular, ^{113}Cd NMR[1] (Otvos & Armitage, 1980; Frey et al., 1985) and X-ray diffraction (Furey et al., 1986; Collett & Stout, 1987) results have delineated the presence of two metal–thiolate clusters in fully loaded mammalian MT: a tetranuclear cluster (cluster A) in the α domain and a trinuclear cluster in the β domain (cluster B). Recently, Mössbauer spectroscopy has been used to establish the nature of the Fe(II)–thiolate clusters in Fe^{II}_4–MT and Fe^{II}_7–MT (Ding et al., 1988). The results provide convincing evidence for the presence of a tetranuclear cluster comprising four high-spin ($S = 2$), tetrahedrally coordinated Fe(II) ions that are antiferromagnetically coupled to give an $S = 0$ ground state. However, the Mössbauer analysis failed to confirm the presence of a second metal–thiolate cluster in fully loaded Fe(II)-substituted MT. Instead, the remaining three iron atoms were found in magnetically isolated sites with properties indicative of monomeric, high-spin ($S = 2$) Fe(II) centers, tetrahedrally coordinated by thiolate ligands.

In order to characterize further the nature and assembly of the Fe(II)–thiolate centers in Fe(II)–MT, we have conducted variable-temperature (1.5–100 K) MCD and EPR[1] studies of samples with varying levels of Fe(II) ion incorporation. The utility of low-temperature MCD spectroscopy as an optical probe for paramagnetic iron–sulfur centers in biology has been well documented (Johnson, 1988; Johnson et al., 1982). Paramagnetic metal centers invariably give rise to temperature-dependent MCD bands that increase in intensity by up to 70-fold on going from room temperature to liquid He temperature. In contrast, diamagnetic metal centers

† This work was supported by grants from the National Science Foundation (DMB8796212) and the National Institutes of Health (GM33806). M.K.J. is the recipient of an Alfred P. Sloan Foundation fellowship.
* Author to whom correspondence should be addressed.

[1] Abbreviations: MT, metallothionein; apoMT, apometallothionein; MCD, magnetic circular dichroism; EPR, electron paramagnetic resonance; NMR, nuclear magnetic resonance; Rd, rubredoxin.

0006-2960/89/0428-3982$01.50/0

exhibit temperature-independent MCD spectra. Consequently, the MCD spectrum of a multicomponent metalloprotein at liquid He temperatures is usually dominated by contributions from paramagnetic centers, and variable-temperature studies provide a means of deconvoluting the spectra of diamagnetic and paramagnetic chromophores. The technique is most informative in conjunction with parallel EPR studies. However, prior to this investigation, no EPR signals had been observed for Fe(II)–MT (Good & Vašák, 1986). Here we report EPR signals indicative of an $S = 2$ ground state at all stages of Fe(II) incorporation. Together with low-temperature MCD data, these results afford new insights into the electronic and magnetic properties of the paramagnetic Fe(II)–thiolate centers in Fe(II)–MT. The conclusions are at variance with the interpretation of the Mössbauer results for fully loaded Fe(II)–MT (Ding et al., 1988) but in accord with the picture that has emerged for the binding of divalent metal ions by mammalian MT.

Experimental Procedures

Lyophilized apometallothionein, prepared from rabbit liver metallothionein isoform I, was generously supplied by Dr. Milan Vašák. *Desulfovibrio gigas* rubredoxin (Rd)[1] was kindly supplied by Drs. José and Isabel Moura. Ultradry oxygen-free $FeCl_2$ (99.999%) was obtained from Johnson-Matthey. All experimental procedures were performed under an inert argon atmosphere in a Vacuum Atmospheres glovebox (<1 ppm O_2).

Solutions of apoMT were prepared by dissolving solid apoMT in 0.1 M HCl to a concentration of approximately 1 mM (i.e., 6 mg/mL). The final concentration of the apoMT stock solution was determined by measuring the absorbance at 220 nm, with $\epsilon_{220} = 7.9$ mg^{-1} mL cm^{-1} (Vašák & Kägi, 1981) and a molecular mass of 6100 kDa. Iron was added to apoMT as a concentrated stock solution of $FeCl_2$ in 0.1 M HCl. Binding of iron to apoMT occurred as the pH was increased to 8.5 by the addition of Tris base. Samples for MCD spectroscopy were diluted with an equal volume of 50 mM Tris-HCl buffer, pH 7.9, followed by dilution with glycerol to give a 1:1 buffer–glycerol solvent which gave optical-quality glasses on freezing. The presence of glycerol did not alter either the UV–visible or EPR spectra. A 1 mM solution of $FeCl_2$, prepared by substituting water for apoMT solution in the above procedure, was used to ascertain the spectroscopic properties of free Fe(II) ions. Rubredoxin was reduced by anaerobic addition of a 10-fold stoichiometric excess of sodium dithionite taken from a 100 mM stock solution in 100 mM Tris-HCl, pH 8.0.

The MCD spectrometer and the experimental protocols for measuring spectra in the 180–1000-nm region at temperatures between 1.5 and 300 K and magnetic fields up to 5 T have been described elsewhere (Kowal et al., 1988; Johnson, 1988). MCD samples were placed in anaerobic 0.1-cm quartz cells. Sample concentrations, temperatures, and magnetic fields are reported in the figure legends. MCD spectra are corrected for natural CD and expressed as the difference in the molar extinction coefficients for left and right circularly polarized light, $\Delta\epsilon$. Any depolarization of the light beam by the sample was corrected for by measuring the natural CD of a standard sample of D-tris(ethylenediamine)cobalt(III) chloride placed in the optical path before and after positioning of the MCD sample. MCD magnetization plots were constructed by monitoring the MCD intensity at several fixed temperatures as a function of the magnetic field strength. The data were corrected for temperature-independent contributions from diamagnetic species by extrapolating plots of MCD intensities versus inverse temperature to infinite temperature and subtracting a proportional correction at each field. Data are plotted as percent (%) magnetization against $\beta B/2kT$, where percent magnetization is the percentage of the MCD intensity relative to saturation at the maximum magnetic field used in these investigations, i.e., 4.5 T, β is the Bohr magneton, B is the magnetic field strength, k is the Boltzmann constant, and T is the absolute temperature.

A Bruker ER-220D EPR spectrometer interfaced to a Bruker ESP1600 computer was used to record X-band EPR spectra. EPR samples were frozen in 3 mm i.d. quartz tubes and stored in liquid nitrogen. Low-temperature spectra were obtained by placing samples in an Oxford Instruments ESR-9 cryostat positioned in a TE_{102} cavity. UV–visible spectra were recorded in septum-capped 0.1-cm quartz cells with a Hewlett-Packard 8452A diode-array spectrophotometer.

Results

UV–Visible Absorption and MCD Studies. Room-temperature absorption spectra and low-temperature MCD spectra (4.2 K and 4.5 T) for Fe(II)–MT samples with Fe(II)/apoMT ratios between 1.3 and 10 are shown in Figure 1. Studies of $FeCl_2$ in the same medium used for the MT studies showed that excess Fe(II) ion in samples with up to 13 equiv of Fe(II) does not contribute significantly to either the absorption or MCD spectra in the spectral regions investigated. Thus it was not necessary to remove excess Fe(II) ions prior to spectroscopic studies. The room-temperature absorption spectra are in good agreement with those previously reported by Good and Vašák (1986). For Fe(II)/MT ratios below 4, the absorption spectra closely resemble those observed for reduced Rd (Eaton & Lovenberg, 1973) and other monomeric tetrahedral tetrathiolate–Fe(II) complexes (Anglin & Davison, 1975; Lane et al., 1977; Ueyama et al., 1985). These spectra are characterized by a well-resolved band at ~312 nm and a shoulder to lower energy at ~340 nm. While specific assignments are not possible without knowledge of the energies of excited-state ligand orbitals, they are attributed to Fe(II) → S charge-transfer transitions (Bair & Goddard, 1978). In accord with previous studies (Good & Vašák, 1986), the intensity of these bands increases linearly with the Fe(II)/apoMT ratio up to 4 equiv of Fe(II), suggesting the formation of noninteracting mononuclear Fe(II) centers tetrahedrally coordinated by cysteinyl S. Above 4 equiv of Fe(II), the absorption intensity no longer increases proportionately with the Fe(II)/apoMT ratio. Rather, the absorption broadens and becomes red shifted, with no further significant changes above 7 equiv of Fe(II). On the basis of comparisons with well-defined mononuclear and polynuclear Fe(II)–thiolate complexes, Good and Vašák (1986) attributed this behavior to the formation of Fe(II)–thiolate clusters containing bridging thiolates in fully loaded Fe_7–MT.

Low-temperature MCD spectra for the samples used for the UV–visible absorption studies are presented in Figure 1. In each case the spectrum is temperature dependent, see below, and as such, the dominant transitions must originate from paramagnetic chromophores. With this in mind, it is apparent that the changes in the MCD spectra are in accord with the above interpretation of the UV–visible absorption data. The 4.2 K MCD intensity is proportional to the Fe(II)/apoMT ratio and the form of the spectrum is unchanged up to 4 equiv of Fe(II), indicating that the first four Fe(II) ions go into sites with similar magnetic properties. The spectrum consists of an intense positively signed band at 334 nm and negatively signed bands at 305 and 280 (shoulder) nm in the Fe(II) → S charge-transfer region. In addition there are two weak positive bands centered at 440 and 530 nm (not clearly visible

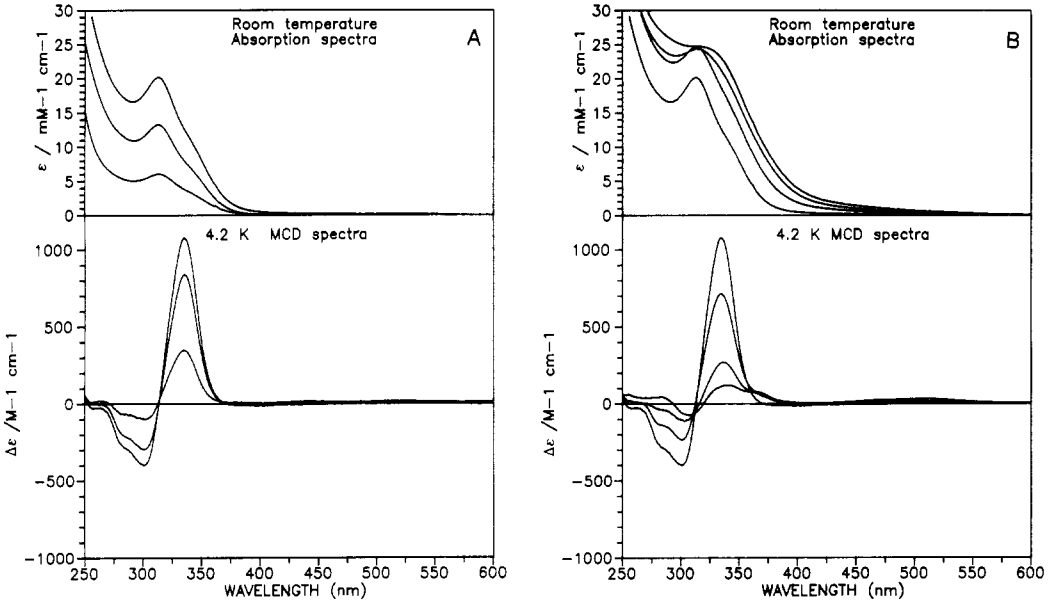

FIGURE 1: Room-temperature absorption and 4.2 K MCD spectra of Fe(II)–MT samples as a function of Fe(II)/apoMT ratio. All samples contained 50% (v/v) glycerol and were prepared as described under Experimental Procedures. Final concentrations ranged from 70 to 300 μM on the basis of the apoMT concentration. Conditions of measurement for MCD spectra: magnetic field, 4.5 T; temperature, 4.2 K; path length, 0.1 cm. (Panel A) Fe(II)/apoMT ratios: 1.3, 2.7, and 4.0. Absorption and MCD spectra both increase in intensity with increasing Fe(II)/apoMT ratio. (Panel B) Fe(II)/apoMT ratios: 4.0, 6.0, 6.9, and 10. Absorption intensity at 350 nm increases with increasing Fe(II)/apoMT ratio; MCD intensity at 335 nm decreases with increasing Fe(II)/apoMT ratio.

on the scale used in Figure 1) that are believed to originate from spin-forbidden quintet to triplet d–d transitions (Bair & Goddard, 1978). The progressive decrease in the 4.2 K MCD intensity at 334 nm for Fe(II)/apoMT ratios > 4 suggests loss of paramagnetic centers, which is consistent with the formation of clusters with antiferromagnetically coupled high-spin Fe(II) centers. Samples with 10 and 13 equiv of Fe(II) ion exhibited identical 4.2 K MCD spectra, and by extrapolation, the changes in the spectra were found to be complete at around 7 equiv. Of most importance is the observation that the low-temperature MCD spectrum of fully loaded Fe(II)–MT is quite distinct in both form and intensity to that observed for samples with less than 4 equiv of Fe(II). It consists of positive maxima at 285, 340, and 365 nm and a negative band at 308 nm, in the Fe(II) → S charge-transfer region, and a broad positive band centered at 500 nm in the quintet to triplet d–d region.

To facilitate more detailed comparison of the MCD characteristics of MT with maximal and low levels of Fe(II) incorporation, spectra b and c of Figure 2 show the temperature dependence of samples containing 1.3 and 10 equiv of Fe(II) ion, respectively. Analogous MCD data are also presented for reduced *D. gigas* Rd, Figure 2a. This serves to illustrate the type of spectra to be expected for a monomeric Fe(II) center with tetrahedral cysteinyl coordination. The Rd spectra are in good agreement with the published data (290–360 nm, 5 T, 17.5–48 K) (Johnson et al., 1982) and greatly extend the wavelength and temperature range. There is a close correspondence between the low-temperature MCD spectra of $Fe_{1.3}$–MT and that of reduced *D. gigas* Rd. While the spectra for the former are broader and less well resolved, probably as a result of some heterogeneity in the multiple coordination sites, the major bands have the same sign and occur at identical wavelengths. Hence, the low-temperature MCD data support the view that the first four Fe(II) ions go into noninteracting monomeric sites with each having tetrahedral cysteinyl coordination. Extrapolation to infinite temperature indicates negligible temperature-independent contributions to the MCD spectrum of $Fe_{1.3}$–MT. In contrast, a large temperature-independent MCD component is apparent for Fe_{10}–MT. Indeed, the temperature-independent component dominates the 89.5 K MCD spectrum. Therefore, the low-temperature MCD is a superposition of transitions originating from both paramagnetic and diamagnetic centers. Diamagnetic behavior is clearly a manifestation of cluster formation. In accord with this, the temperature-independent MCD envelope of Fe(II) → S charge-transfer transitions is broadened and shifted to lower energy compared to that of monomeric tetrathiolate–Fe(II) centers, as would expected for a cluster involving both terminal and bridging thiolates. The MCD spectrum corresponding to the paramagnetic center was obtained by subtracting the spectra at 89.5 K from that at 4.22 K, see Figure 2d. The intensity and form of the spectrum can only be reconciled with those of the paramagnetic Fe(II)–thiolate cluster, with the positive bands at 335 and 365 nm corresponding to predominantly Fe(II) → S(terminal) and Fe(II) → S(bridging) charge transfer, respectively.

In an attempt to probe the magnetic properties of paramagnetic Fe(II)–thiolate centers in Fe(II)–MT, MCD magnetization curves (Thomson & Johnson, 1980) were constructed for the most intense bands. Figure 3 shows magnetization plots for the reduced Rd, the monomeric Fe(II)–thiolate center in $Fe^{II}_{1.3}$–MT, and the paramagnetic Fe(II)–thiolate cluster in Fe^{II}_{10}–MT. In each case the data obtained at different temperatures lie on separate curves, leading to "nested" plots. Such behavior is characteristic of ground states with $S > {}^1/_2$ that are subject to zero-field splitting and is a consequence of thermal population and field-induced mixing of zero-field components (Thomson & Johnson, 1980; Johnson et al., 1982; Whittaker & Solomon, 1988). Detailed theoretical analyses of these magnetization curves are in progress, and the results will be reported elsewhere. Here, it is sufficient to note the close correspondence in the magnetization data shown in Figure 3, since this attests to an $S = 2$ ground state with similar zero-field splitting parameters in each instance. Spin Hamiltonian analyses of Mössbauer data for the $S = 2$ tetrathiolate–Fe(II) centers in reduced Rd (Winkler et al., 1979), $[Fe(SPh)_4]^{2-}$ (Trautwein

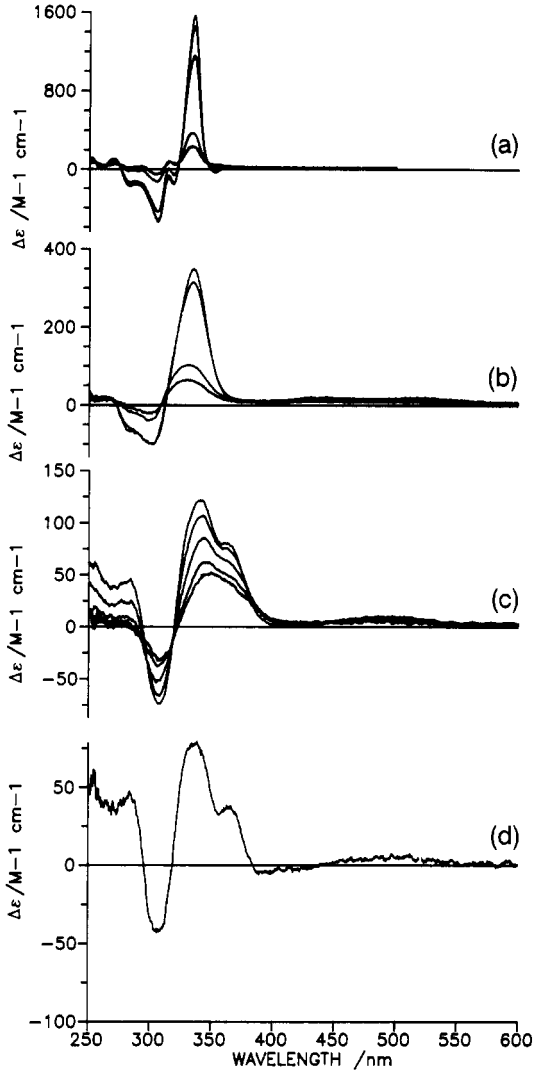

FIGURE 2: Temperature dependence of the MCD spectra of dithionite-reduced *D. gigas* Rd, $Fe^{II}_{1.3}$–MT, and Fe^{II}_{10}–MT. Fe(II)–MT samples contained 50% (v/v) glycerol and were prepared as described under Experimental Procedures. Conditions of measurement: magnetic field, 4.5 T; path length, 0.1 cm. In all cases MCD intensity decreases with increasing temperature. (a) Rubredoxin. Protein concentration was 64 μM in 50 mM Tris-HCl buffer, pH 7.9, with 50% (v/v) glycerol. Temperatures were 1.75, 4.22, 9.9, 50, and 90 K. (b) $Fe^{II}_{1.3}$–MT. Protein concentration was 243 μM. Temperatures were 4.22, 8.8, 50, and 90 K (the spectrum recorded at 1.73 K overlays that at 4.22 K and is not shown for clarity). (c) Fe^{II}_{10}–MT. Sample concentration was 248 μM. Temperatures were 4.22, 9.0, 20, 50, and 90 K (the spectrum recorded at 1.60 K overlays that at 4.22 K and is not shown for clarity). (d) Temperature-dependent component of the MCD spectrum of Fe^{II}_{10}–MT, generated by subtraction of the 90 K spectrum from the 4.22 K spectrum.

et al., 1985), and Fe^{II}_4–MT (Ding et al., 1988) do indeed indicate very similar zero-field splitting parameters, i.e., $D \sim 8$ cm^{-1} and $E/D \sim 0.28$. Therefore, on the basis of the close correspondence in the magnetization data, we tentatively conclude that the paramagnetic Fe(II)–thiolate cluster in fully loaded Fe(II)–MT also has an $S = 2$ ground state with $D > 0$.

EPR Studies. X-band EPR spectra for the samples used in the MCD and absorption studies are shown in Figure 4. During titration with Fe(II) ion, a broad resonance ("$g = 10$" signal) appears to low field (maximum, $g = 12$; crossover, $g = 10$; minimum, $g = 7.5$). The resonance increases in intensity up to approximately 4 equiv of Fe(II), remains almost constant between 4 and 6 equiv, and undergoes a marked decrease between 6 and 7 equiv. It is, however, still present in fully

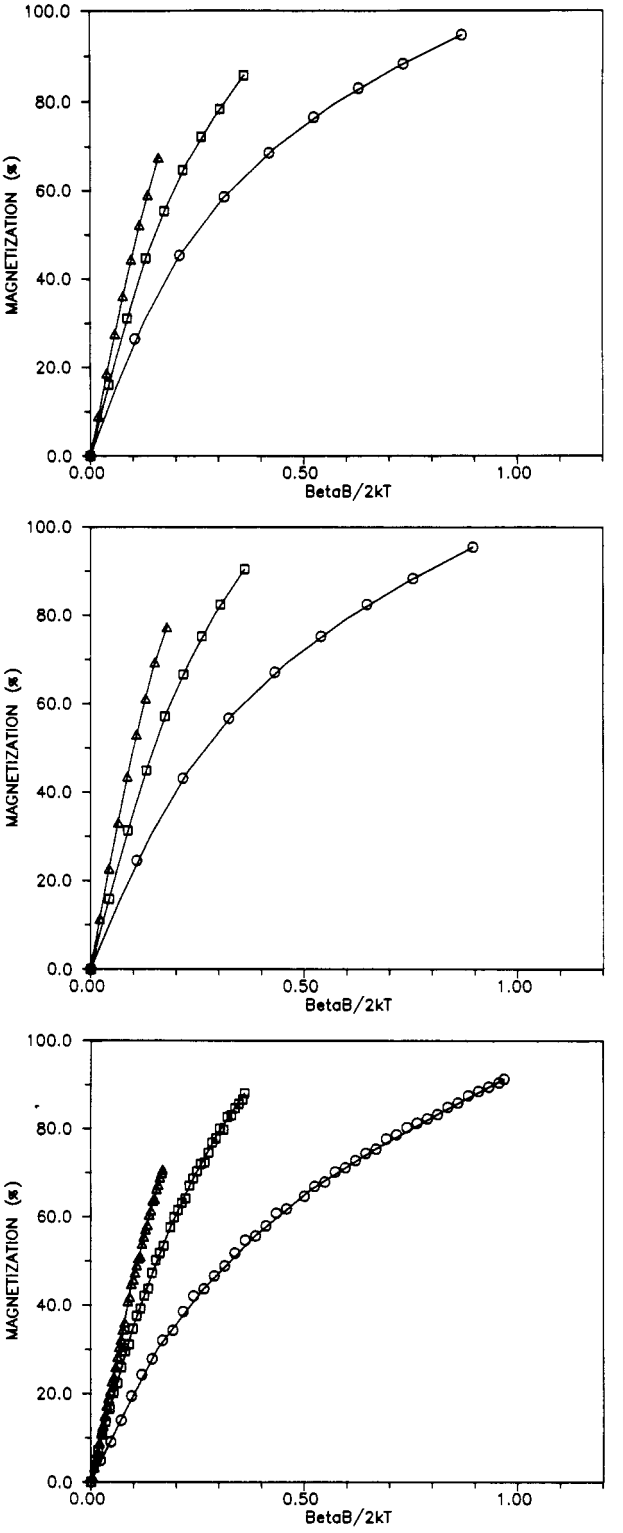

FIGURE 3: MCD magnetization plots for dithionite-reduced *D. gigas* Rd, $Fe^{II}_{1.3}$–MT, and Fe^{II}_{10}–MT. (Upper panel) Dithionite-reduced *D. gigas* Rd at 334 nm. Sample conditions are given in Figure 2. Magnetic fields were between 0 and 4.5 T. Temperatures were (○) 1.75, (□) 4.22, and (△) 8.5 K. (Middle panel) Fe^{II}_1–MT at 334 nm. Sample conditions are given in Figure 2. Magnetic fields were between 0 and 4.5 T. Temperatures were (○) 1.70, (□) 4.22, and (△) 8.5 K. (Lower panel) Fe^{II}_{10}–MT at 335 nm. Sample conditions are given in Figure 2. Magnetic fields were between 0 and 4.5 T. Temperatures were (○) 1.57, (□) 4.22, and (△) 9.0 K. Solid lines are best fits with a cubic spline function.

loaded MT. Above 7 equiv an additional new positive feature progressively appears at around 100 mT. This is attributed to free Fe(II) ions, since it is observed in the EPR spectrum

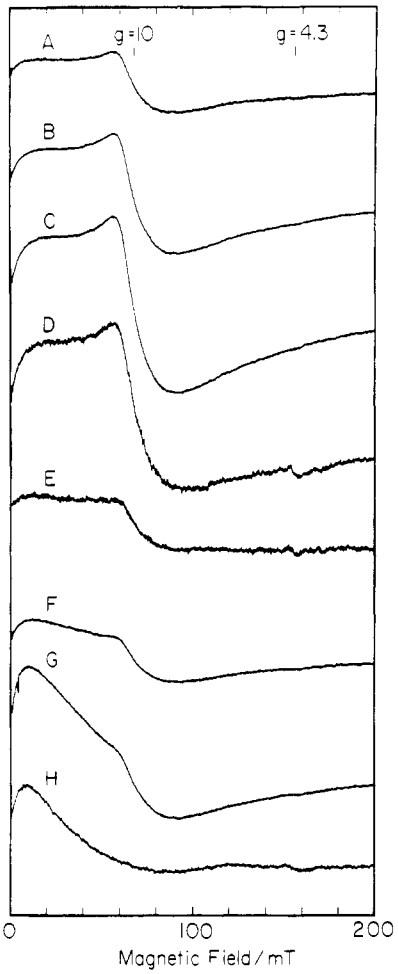

FIGURE 4: X-band EPR spectra of Fe(II)–MT samples. Conditions of measurement: temperature, 4.2 K; microwave frequency, 9.41 GHz; microwave power, 20 mW; modulation frequency, 100 MHz; modulation amplitude, 1.26 mT. Spectra have been normalized to a MT concentration of 0.70 mM and receiver gain of 5×10^5. Fe(II)/apoMT ratios: (A) 1.3, (B) 2.7, (C) 4.0, (D) 6.0, (E) 6.9, (F) 10.0, and (G) 13.7. (H) is the EPR spectrum of 1 mM $FeCl_2$ in the same medium used for the Fe(II)–MT samples.

of $FeCl_2$ in the same medium used for the MT studies, see Figure 4H. Similar EPR spectra have been observed for a number of transition metal centers exhibiting $S = 2$ ground states (Hagen, 1982; Hagen et al., 1985; Hendrich & Debrunner, 1988; Werth et al., 1989) and have been attributed to the $\Delta M_s = 4$ transition within the $M_s = \pm 2$ doublet of the zero-field components. Consequently, the observation of this resonance in fully loaded Fe(II)–MT is in accord with an $S = 2$ ground state for the paramagnetic Fe(II)–thiolate cluster in fully loaded Fe(II)–MT.

The form of the EPR resonance in Fe(II)–MT is almost identical with that observed in monomeric Fe(II)–alkylthiolate model complexes (Werth et al., 1989). Moreover, the spectra show analogous temperature dependence behavior. Plots of the signal amplitude versus $1/T$ for the $Fe^{II}_{1.3}$–MT and Fe^{II}_{10}–MT show Curie law behavior over the temperature range 4.2–16 K (data not shown). Given the assignment of the resonance, such behavior would only be expected for an almost axial $S = 2$ ground state with large negative D, leaving the $M_s = \pm 2$ doublet lowest in energy and split in zero field by <0.3 cm^{-1}. Thus the picture of the zero-field splitting that emerges from analysis of the EPR data is quite different to that inferred from the MCD and Mössbauer data for both the monomeric Fe(II)–thiolate center and the paramagnetic Fe(II)–thiolate cluster in Fe(II)–MT. The likely reasons for this apparent inconsistency are discussed below.

Discussion

The results presented here provide new information concerning the assembly and properties of the Fe(II)–thiolate centers in Fe(II)–MT. The low-temperature MCD and EPR studies concur with the previous absorption and room-temperature MCD studies (Good & Vašák, 1986) in finding that MT binds a maximum of seven Fe(II) ions. However, in contrast to the Mössbauer studies which reported a diamagnetic tetrameric Fe(II)–thiolate cluster and three noninteracting monomeric tetrahedral Fe(II)–thiolate centers (Ding et al., 1988), the low-temperature MCD and EPR data are best interpreted in terms of Fe(II)–thiolate clusters with diamagnetic ($S = 0$) and a paramagnetic ($S = 2$) ground states in fully loaded Fe(II)–MT. As previously noted (Ding et al., 1988), the Mössbauer result is surprising in that there are insufficient cysteine residues to coordinate three Fe(II) ions independently, in addition to an adamantane-type tetrameric Fe(II)–thiolate cluster. We have considered two possible explanations for the discrepancy between the Mössbauer and the combined EPR and MCD results. First, since the MCD magnetization curves suggest similar zero-field splitting parameters for the $S = 2$ ground states of the monomeric and paramagnetic cluster species, could they exhibit indistinguishable magnetic Mössbauer spectra? This seems highly improbable because antiferromagnetic exchange coupling would be expected to result in different effective magnetic hyperfine values (A values) for each Fe in the cluster, since they are referred to the ground-state system spin of the coupled system rather than the spins of the constituent Fe atoms. Second, the sample used for Mössbauer studies was not fully loaded, i.e., Fe(II)/apoMT ratio <7. As discussed below, the results presented herein, coupled with available data for divalent metal ion binding and cluster assembly at pH >8, are more consistent with this explanation.

Recent investigations of Cd(II) and Co(II) binding to MT have clarified the conflicting reports concerning the pathway of cluster formation, by finding the process to be pH dependent (Vašák, 1988; Good et al., 1988). At physiological pH, the binding is sequential and cooperative with the initial event involving formation of the tetranuclear cluster in the α domain for metal/apoMT ratios < 4. In contrast at pH 8.6, the metal ions go into rapidly exchanging noninteracting monomeric sites for metal/apoMT ratios < 4. Preferential formation of the tetranuclear cluster in the α domain ensues only for ratios > 4. In accord with this, all spectroscopic studies of Fe(II)–MT (pH 8.3–8.5) with Fe(II)/apoMT ratios ≤ 4 concur in finding monomeric tetrathiolate–Fe(II) sites as the dominant species. Changes in the magnetic and electronic properties are clearly indicative of cluster formation for Fe(II)/apoMT ratios > 4. However, the low-temperature MCD and EPR data both indicate that a substantial proportion of the Fe(II) ions still resides in monomeric Fe(II) sites in Fe^{II}_6–MT. For example, on the basis of the intensity of the temperature-dependent MCD band at 334 nm, we estimate that 2.5 ± 0.5 of the Fe(II) ions are in noninteracting monomeric sites in Fe^{II}_6–MT. Given the preferential buildup of the tetranuclear cluster in the α domain that has been established for other divalent metals, the majority of the remaining Fe is assumed to reside in tetranuclear clusters. Furthermore, by analogy with the magnetic properties of adamantane-type model complexes of the type $[Fe_4(SR)_{10}]^{2-}$ (Whitener et al., 1986), this cluster is expected to have a diamagnetic ($S = 0$) ground state. This being so, the Mössbauer spectrum of Fe^{II}_6–MT would be expected to consist of paramagnetic and diamagnetic subspectra

in a ratio of approximately 3:4, with the paramagnetic component corresponding to that of monomeric and noninteracting high-spin Fe(II) sites. Since these were the Mössbauer characteristics that were reported for Fe^{II}_7–MT by Ding et al. (1988), we consider that an overestimate of the Fe(II)/apoMT ratio offers the best explanation of the discrepancy between the Mössbauer results and those presented herein.

From the above arguments, we assign the cluster with the diamagnetic ($S = 0$) ground state in fully loaded Fe(II)–MT to a tetranuclear species. Consequently, the paramagnetic ($S = 2$) cluster is attributed to a trinuclear species that is assembled in the β domain for Fe(II)/apoMT ratios > 6. This interpretation of the nature of the Fe(II)–thiolate centers in Fe^{II}_7–MT is based primarily on the picture that has emerged from ^{113}Cd NMR studies of Cd_7–MT (Otvos & Armitage, 1980; Frey et al., 1985) and X-ray diffraction studies of Zn_2Cd_5–MT (Furey et al., 1986; Collett & Stout, 1987). A similar cluster composition has also been inferred for Co^{II}_7–MT (Vašák, 1980; Vašák & Kägi, 1981), and recent low-temperature MCD and EPR studies have provided evidence for $S = 0$ and $S = {}^3/_2$ ground states for the tetranuclear and trinuclear clusters, respectively (Dixon & Johnson, 1987). To our knowledge, there are at present no model complexes of the type $[Fe_3(SR)_9]^{3-}$ (six terminal and three bridging thiolates) that would serve as structural analogues of the trinuclear cluster in Fe^{II}_7–MT. Trinuclear clusters of the formula $[Fe_3(SR)_3X_6]^{3-}$ (X = Cl or Br) containing a planar $Fe_3(\mu_2\text{-}SR)_3$ unit have been prepared and characterized (Whitener et al., 1986). These compounds have effective C_2 symmetry and exhibit an $S = 0$ ground state as a result of antiferromagnetic coupling ($J_{12} = J_{13} = -22.5$ cm^{-1}, $J_{23} = -18.7$ cm^{-1}) between the three ($S = 2$) Fe(II) centers. An $S = 2$ ground state would require a coupling scheme with greater differences in the magnetic coupling constants between each pair of Fe atoms and hence a more distorted geometry.

At this juncture it is appropriate to point out an important limitation of the low-temperature MCD and EPR results with respect to the magnetic properties of the trinuclear cluster in Fe(II)–MT. Neither technique permits quantitation of the species that have $S = 2$ ground states. Consequently, the possibility that only a fraction of trinuclear clusters have $S = 2$ ground states, with the remainder having $S = 0$ ground states, cannot be excluded. Indeed, ^{113}Cd NMR studies of Cd_7–MT have revealed considerable conformational flexibility, particularly for the trinuclear cluster in the β domain (Nettesheim et al., 1985; Vašák et al., 1985; Otvos et al., 1987). Moreover, the act of freezing itself may alter the relative contributions of different structural forms of this cluster. At best we can conclude that some or all of the trinuclear clusters in frozen solutions of Fe^{II}_7–MT exist in a form with an $S = 2$ ground state.

Finally, we turn our attention to the apparent inconsistency in the EPR results on the one hand and the Mössbauer and MCD results on the other with respect to the sign and nature of the zero-field splitting of the $S = 2$ ground states of both the monomeric and trimeric centers. While the arguments presented below are applicable to both the monomeric and trinuclear centers, we will focus the discussion on the former, since Mössbauer data are available for a range of $[Fe(SR)_4]^{2-}$ centers including that in Fe(II)–MT at low Fe(II)/apoMT ratios. By use of the Mössbauer-determined zero-field splitting parameters, $D = 8.0$ cm^{-1} and $E/D = 0.28$, the predicted splitting of the $S = 2$ ground state would preclude the observation of an X-band EPR resonance for the monomeric tetrathiolate–Fe(II) centers in Fe(II)–MT. A $\Delta M_s = 4$ transition would not be possible, since the $M_s = \pm 2$ zero-field doublet is highest in energy and split by ~ 2 cm^{-1}. Furthermore, the two lowest level zero-field components are separated by ~ 4 cm^{-1}. Indeed, no EPR signals have been reported for reduced Rd or $[Fe(SPh)_4]^{2-}$ which have similar zero-field splitting parameters (Winkler et al., 1979; Trautwein et al., 1985). At this point a few comments are appropriate concerning $S = 2$ EPR signals. First, it should be emphasized that theoretical understanding of the broad low-field resonances that are sometimes observed in the EPR spectra of $S = 2$ systems is still emerging [for a recent discussion, see Hendrich and Debrunner (1988)]. In light of this and the absence of suitable standards, it is not possible to determine a reliable estimate of the spin concentration of the $S = 2$ species that is responsible for the EPR signal. Therefore, the most likely explanation for the observation of the $g = 10$ resonance is that it arises from a minor $S = 2$ species with $D < 0$ and small E/D, whereas the low-temperature MCD and Mössbauer studies are monitoring the major $S = 2$ species. Such heterogeneity might be expected in light of the multiplicity of potential binding sites and is consistent with the broadening of the low-temperature MCD spectrum relative to that of reduced Rd.

This conclusion is further substantiated by recent Mössbauer and EPR studies of aqueous solutions of $[Fe(SCH_2CH_2OH)_4]^{2-}$ (Werth et al., 1989). This compound exhibits an EPR spectrum with identical form and temperature dependence to those observed for Fe(II)–MT. Moreover, the Mössbauer studies revealed two species in the aqueous frozen solution. The major species has zero-field parameters analogous to those of reduced Rd and thus cannot be responsible for the EPR resonance. In contrast, the minor species has $D \sim -5$ cm^{-1} and $E/D \sim 0.17$, which results in the $M_s = \pm 2$ doublet lowest in energy and split by 0.3–0.5 cm^{-1}. Such a ground state meets the requirements for the observation of an EPR resonance at X-band frequencies within the experimental error of the zero-field splitting parameters. This result indicates that there are at least two distinct stable conformations of this tetrathiolate–Fe(II) complex in aqueous solution. If a similar heterogeneity is indeed the explanation for the observed EPR properties on Fe(II)–MT, then the question of why it was not apparent in the Mössbauer data (Ding et al., 1988) needs to be addressed. Since the heterogeneity in the 4.2 K Mössbauer spectra of this compound was only clearly apparent in the spectra at low applied fields, 0.5 and 1.0 T, the answer probably lies in the fact that Mössbauer data for Fe(II)–MT were only reported at zero applied field and at applied fields > 2.47 T. Clearly, additional Mössbauer studies are called for to address this question of heterogeneity and to characterize further the magnetic properties of the metal clusters in fully loaded Fe(II)–MT.

Acknowledgments

We thank Drs. José and Isabel Moura for providing samples of *D. gigas* rubredoxin. We are especially grateful to Dr. Milan Vašák for providing lyophilized apometallothionein for these investigations, for communicating manuscripts to us prior to publication, and for many helpful discussions.

References

Anglin, J. R., & Davison, A. (1975) *Inorg. Chem. 14*, 234–237.

Bair, A. R., & Goddard, W. A. (1978) *J. Am. Chem. Soc. 100*, 5669–5676.

Collett, S. A., & Stout, C. D. (1987) *Recl. Trav. Chim. Pays-Bas 106*, 182.

Ding, X., Bill, E., Good, M., Trautwein, A. X., & Vašák, M. (1988) *Eur. J. Biochem. 171*, 711–714.

Dixon, B. A., & Johnson, M. K. (1987) *Recl. Trav. Chim. Pays-Bas 106*, 188.

Eaton, E. A., & Lovenberg, W. (1973) in *Iron-Sulfur Proteins* (Lovenberg, W., Ed.) Vol. II, pp 131–162, Academic Press, New York.

Frey, M. H., Wagner, G., Vašák, M., Sørenson, O. W., Neuhaus, D., Wörgötter, E., Kägi, J. H. R., Ernst, R. R., & Wüthrich, K. (1985) *J. Am. Chem. Soc. 107*, 6847–6851.

Furey, W. F., Robbins, A. H., Clancy, L. L., Winge, D. R., Wang, B. C., & Stout, C. D. (1986) *Science (Washington, D.C.) 231*, 704–710.

Good, M., & Vašák, M. (1986) *Biochemistry 25*, 8353–8356.

Good, M., Hollenstein, R., Sadler, P. J., & Vašák, M. (1988) *Biochemistry 27*, 7163–7166.

Hagen, W. R. (1982) *Biochim. Biophys. Acta 708*, 82–89.

Hagen, W. R., Dunham, W. R., Johnson, M. K., & Fee, J. A. (1985) *Biochim. Biophys. Acta 828*, 369–374.

Hamer, D. H. (1986) *Annu. Rev. Biochem. 55*, 913–995.

Hendrich, M. P., & Debrunner, P. G. (1988) *J. Magn. Reson. 78*, 133–141.

Johnson, M. K. (1988) in *Metal Clusters in Proteins* (Que, L., Jr., Ed.) pp 326–342, ACS Symposium Series 372, American Chemical Society, Washington, DC.

Johnson, M. K., Robinson, A. E., & Thomson, A. J. (1982) in *Iron Sulfur Proteins* (Spiro, T. G., Ed.) pp 367–406, Wiley, New York.

Kägi, J. H. R., & Vallee, B. L. (1961) *J. Biol. Chem. 236*, 2435–2442.

Kägi, J. H. R., Vašák, M., Lerch, K., Gilg, D. E. O., Hunziker, P., Bernhard, W. R., & Good, M. (1984) *EHP, Environ. Health Perspect. 54*, 93–103.

Kojima, N., Berger, C., Vallee, B. L., & Kägi, J. H. R. (1976) *Proc. Natl. Acad. Sci. U.S.A. 73*, 3413–3417.

Kowal, A. T., Zambrano, I. C., Moura, I., Moura, J. J. G., LeGall, J., & Johnson, M. K. (1988) *Inorg. Chem. 27*, 1162–1166.

Lane, R. W., Ibers, J. A., Frankel, R. B., Papaefthymiou, G. C., & Holm, R. H. (1977) *J. Am. Chem. Soc. 99*, 84–98.

Margoshes, M., & Vallee, B. L. (1957) *J. Am. Chem. Soc. 79*, 4813–4814.

Nettesheim, D. G., Engeseth, H. R., & Otvos, J. D. (1985) *Biochemistry 24*, 6744–6751.

Nielson, K. B., Atkin, C. L., & Winge, D. R. (1985) *J. Biol. Chem. 260*, 5342–5350.

Nordberg, M., & Kojima, Y. (1979) in *Metallothionein* (Käji, J. H. R., & Nordberg, M., Eds.) pp 41–124, Birkhäuser Verlag, Basel.

Otvos, J. D., & Armitage, I. M. (1980) *Proc. Natl. Acad. Sci. U.S.A. 77*, 7094–7098.

Otvos, J. D., Engeseth, H. R., Nettesheim, D. G., & Hilt, C. R. (1987) in *Proceedings of the 2nd International Meeting on Metallothionein* (Kägi, J. H. R., & Kojima, Y., Eds.) pp 171–178, Birkhäuser Verlag, Basel.

Thomson, A. J., & Johnson, M. K. (1980) *Biochem. J. 191*, 411–420.

Trautwein, A. X., Bill, E., Bläs, R., Lauer, S., & Winkler, H. (1985) *J. Chem. Phys. 82*, 3582–3593.

Ueyama, N., Nakata, M., Fuji, M. A., Terakawa, T., & Nakamura, A. (1985) *Inorg. Chem. 24*, 2190–2196.

Vašák, M. (1980) *J. Am. Chem. Soc. 102*, 3953–3955.

Vašák, M. (1988) in *Metal Ion Homeostasis: Molecular Biology and Chemistry* (Winge, D. R., & Hamer, D. H., Eds.) UCLA Symposia on Molecular and Cellular Biology, New Series, Vol. 98, Liss, New York (in press).

Vašák, M., & Kägi, J. H. R. (1981) *Proc. Natl. Acad. Sci. U.S.A. 78*, 6709–6713.

Vašák, M., Nicholson, J. K., Hawkes, G. E., & Sadler, P. J. (1985) *Biochemistry 24*, 740–747.

Werth, W. T., Kurtz, D. M., Jr., Howes, B. D., & Huynh, B. H. (1989) *Inorg. Chem.* (in press).

Whitener, M. A., Bashkin, J. K., Hagen, K. S., Girerd, J.-J., Gamp, E., Edelstein, N., & Holm, R. H. (1986) *J. Am. Chem. Soc. 108*, 5607–5602.

Whittaker, J. W., & Solomon, E. I. (1988) *J. Am. Chem. Soc. 110*, 5329–5339.

Winkler, H., Schultz, C., & Debrunner, P. G. (1979) *Phys. Lett. 69A*, 360–363.